Electrical transport and magnetic properties of $(Ce_{1-x}Gd_x)Pt_2Si_2$ $(0 \leq x \leq 1)$

2003 J. Phys.: Condens. Matter 15 3767

(http://iopscience.iop.org/0953-8984/15/22/311)

INSTITUTE OF PHYSICS PUBLISHING JOURNAL OF PHYSICS: CONDENSED MATTER

J. Phys.: Condens. Matter **15** (2003) 3767–3777 PII: S0953-8984(03)60515-1

Electrical transport and magnetic properties of $(Ce_{1-x}Gd_x)Pt_2Si_2$ $(0 \leqslant x \leqslant 1)$

M B Tchoula Tchokonté[1], P de V du Plessis[1] and D Kaczorowski[2]

[1] f-Electron Magnetism and Heavy-Fermion Physics Research Programme, School of Physics, University of the Witwatersrand, Private Bag 3, PO Wits 2050, Johannesburg, South Africa
[2] Institute of Low Temperature and Structure Research, Polish Academy of Sciences, PO Box 1410, 50-950 Wroclaw, Poland

E-mail: tchoula@physnet.phys.wits.ac.za

Received 6 March 2003, in final form 11 April 2003
Published 23 May 2003
Online at stacks.iop.org/JPhysCM/15/3767

Abstract

Results of electrical resistivity, magnetization and susceptibility measurements are reported for the pseudo-ternary alloys $(Ce_{1-x}Gd_x)Pt_2Si_2$. The end-members of the alloy series are the non-magnetic Kondo lattice compound $CePt_2Si_2$ and the antiferromagnet $GdPt_2Si_2$. The resistivity results reveal a rapid evolution to Kondo behaviour beyond small Ce substitution in $GdPt_2Si_2$ (for $1 - x \geqslant 0.2$). Coherent Kondo scattering is observed for larger Ce substitution ($1 - x \geqslant 0.75$). The low-temperature resistivity of $CePt_2Si_2$ in the coherent state is dominantly a T^2 Fermi-liquid behaviour. The magnetization results suggest metamagnetic behaviour at Gd-rich concentrations. From the susceptibility results, the Gd and Ce moments seem to contribute independently to the magnetism of the alloy samples.

1. Introduction

The structural properties of several RT_2Si_2 compounds (R = the rare-earth elements including Ce and T = 3d, 4d or 5d elements) have been reviewed by Rogl [1]. Most of these compounds crystallize in the ordered tetragonal $ThCr_2Si_2$-type structure with space group $I4/mmm$. However, $CePt_2Si_2$, which is a parent compound in the present study, is an exception. Several authors [1–5] report that $CePt_2Si_2$ crystallizes in the tetragonal $CaBe_2Ge_2$-type structure with space group $P4/nmm$. $GdPt_2Si_2$ was reported to exist in a variety of structures [1] including a disordered $ThCr_2Si_2$ structure [6], but in his review article Rogl indicates that it has the $CaBe_2Ge_2$-type structure.

Resistivity [5, 7, 8], magnetic susceptibilty [3, 5, 7] and specific heat [5, 7] measurements establish $CePt_2Si_2$ as a Kondo lattice compound. Specific heat, C_p, measurements have been interpreted in the single-impurity model of Rajan [9] with $J = 1/2$ and a Kondo temperature $T_K = 70$ K. Resistivity data, $\rho(T)$, on a polycrystalline $CePt_2Si_2$ sample

as reported by Gignoux *et al* [5], show a Kondo-like increase in $\rho(T)$ upon cooling from room temperature, culminating in a peak at a temperature $T_{max} = 76$ K, and followed by a marked decrease towards low temperatures. This behaviour for $\rho(T)$ was confirmed in single-crystal studies [8, 10, 11], which also indicate a strong anisotropy. Recent studies of C_p and $\rho(T)$ at low temperatures on a single crystal of $CePt_2Si_2$ indicate a possible non-Fermi-liquid (NFL) ground state for this compound, while μSR measurements indicate the absence of long-range magnetic order down to 60 mK [12]. It has indeed already been indicated earlier for polycrystalline samples that $\rho(T)$ exhibits Fermi-liquid behaviour between 4 and 10 K and tends to a linear temperature dependence below 4 K [7], characteristic of NFL behaviour. Studies of $C_p(T)$ [7, 12] confirm the occurrence of Fermi-liquid behaviour above 15 K, but indicate coherence effects at lower temperatures which seem to correspond to the NFL behaviour observed in a similar temperature region in the $\rho(T)$ data. Magnetic susceptibility measurements, $\chi(T)$, on polycrystalline $CePt_2Si_2$ follow a Curie–Weiss behaviour above 150 K, with $-\theta_p = 86$ K and with $\mu_{eff} = 2.57\ \mu_B$ which is close to 2.54 μ_B of the free Ce^{3+} ion [5]. A broad maximum is observed in the $\chi(T)$ curve around 60 K, together with a minimum at ∼20 K followed by an increase towards lower temperatures. Similar behaviour in $\chi(T)$ was also observed in single-crystal studies [12, 13]. Inelastic neutron scattering studies as interpreted in terms of quasi-elastic scattering suggest that the behaviour of $CePt_2Si_2$ is intermediate between that of valence fluctuation and heavy-fermion (HF) compounds [14].

The influence of substituting Ce with La in $CePt_2Si_2$ has been studied through $\rho(T)$ measurements on polycrystalline samples and illustrates the evolution from coherent Kondo behaviour to incoherent Kondo behaviour with decreased Ce concentration [15]. Resistivity, magnetoresistivity and susceptibility studies have been performed on $CePt_2(Si_{1-x}Ge_x)_2$ alloys [16] and the decrease in T_K with increased Ge substitution has been described in terms of the compressible Kondo lattice model [17].

In the present study the influence of substituting Ce with moment-bearing Gd in $CePt_2Si_2$ is investigated using $\rho(T)$, $\chi(T)$ and magnetization, $\sigma(T)$, measurements.

2. Experimental details

Polycrystalline samples of $(Ce_{1-x}Gd_x)Pt_2Si_2$ were synthesized by arc-melting stoichiometric amounts of the constituent elements on a water-cooled copper hearth in a titanium-gettered high-purity argon atmosphere. Elements of the following purity in wt% were used: Ce, 99.98; Gd, 99.99; Pt, 99.97, and Si, 99.9999. The ingots were turned over and remelted three times to improve their homogeneity. X-ray diffraction measurements using a Philips PW18301 powder diffractometer with Cu Kα radiation indicated the phase purity of the samples and the absence of unreacted elements. The diffractograms showed that the two end-compounds $CePt_2Si_2$ and $GdPt_2Si_2$ as well as the complete range of pseudo-ternary $(Ce_{1-x}Gd_x)Pt_2Si_2$ alloys crystallize in the tetragonal $CaBe_2Ge_2$-type structure with space group $P4/nmm$. The observation of the $CaBe_2Ge_2$ structure for our $GdPt_2Si_2$ sample is in agreement with the earlier assignment of this structure to the compound by Rogl [1]. Lattice parameters were calculated using standard regression analyses on 26 well resolved peaks in the powder spectrum of each alloy. The variation of lattice parameters with Gd content x for the alloy series is discussed in section 3.1.

Measurements of $\rho(T)$ were carried out using a standard four-probe DC technique between 4 and 295 K. The samples had a typical cross sectional area $A = 1 \times 1$ mm^2 and a length $\ell = 8$ mm. The uncertainty in the geometrical factor was typically $A/\ell \pm 2\%$. A YEW-type 2854 DC-current source provided a constant excitation current of 100 mA to the samples. The sample and thermocouple voltages were measured using calibrated Hewlett-Packard 3478A

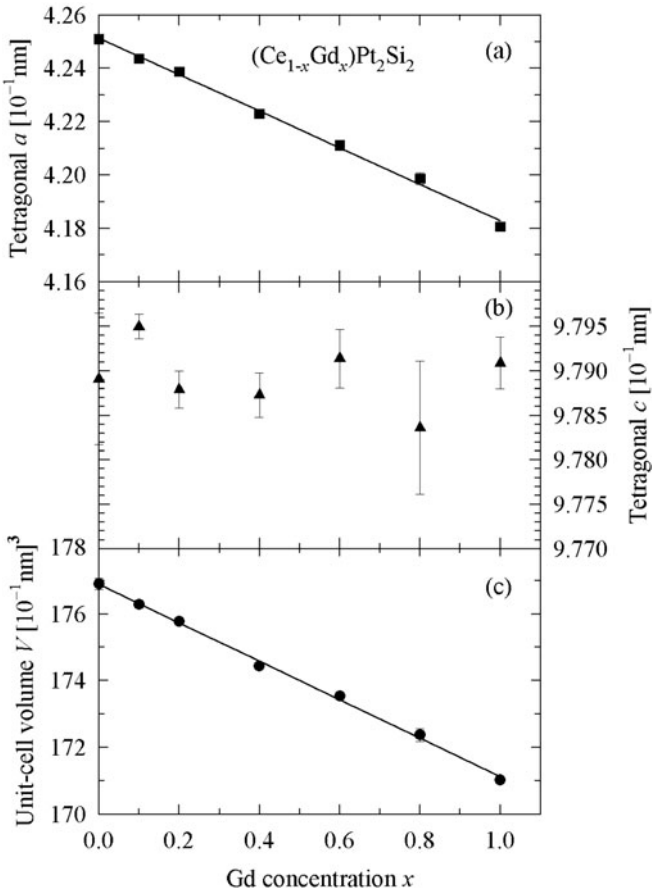

Figure 1. The tetragonal lattice parameters a (a) and c (b) and the unit-cell volume V (c) as a function of Gd concentration x for the $(Ce_{1-x}Gd_x)Pt_2Si_2$ alloy system.

digital voltmeters of 0.1 μV resolution. A Au–0.07 at.% Fe versus chromel thermocouple was used to measure the temperature. Data were collected on a PC using a multiplexer during slow cooling or heating runs in which the temperature changed at a rate of 0.5 K min^{-1}. DC magnetic measurements were performed in the temperature range 1.89–300 K and in applied magnetic fields up to 5 T using a Quantum Design MPMS-5 SQUID magnetometer.

3. Results and discussion

3.1. Lattice parameters

The tetragonal lattice parameters a and c and the unit-cell volume V for the $(Ce_{1-x}Gd_x)Pt_2Si_2$ alloy series are depicted in figure 1. A linear decrease in volume with increasing x is observed, indicating the validity of Vegard's rule. It is observed that the a-axis decreases by 1.6%, but the c-axis only changes by about 0.02%, between $CePt_2Si_2$ and $GdPt_2Si_2$. The decrease in unit-cell volume with increasing Gd content amounts to a volume change of 3.4% between $CePt_2Si_2$ and $GdPt_2Si_2$.

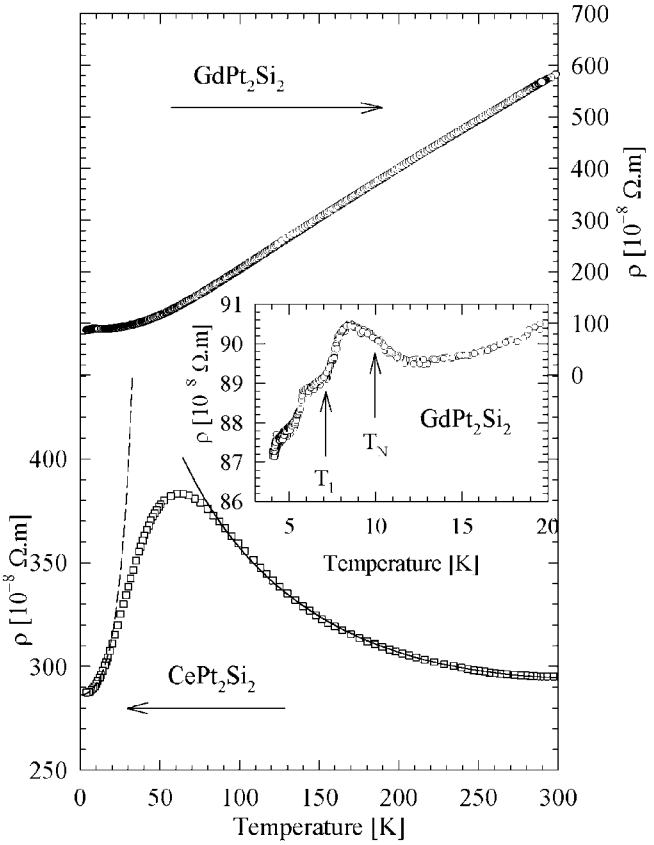

Figure 2. The temperature dependence of the resistivity $\rho(T)$ of $CePt_2Si_2$ exhibiting a $-\ln T$ dependence at higher temperatures (solid curve) and the sum of T^2 and T^5 terms at low temperatures (dashed curve). For $GdPt_2Si_2$ the $\rho(T)$ exhibits normal metallic behaviour for $T > 12$ K. Below 12 K anomalies associated with antiferromagnetic ordering are observed for $GdPt_2Si_2$ as discussed in the text.

3.2. Resistivity

Results of $\rho(T)$ for the two end-compounds $CePt_2Si_2$ and $GdPt_2Si_2$ are compared in figure 2. For $CePt_2Si_2$ the $\rho(T)$ behaviour is typical of a dense Kondo system, showing incoherent Kondo scattering at higher temperatures (solid curve), a well defined peak at 63 K and a dominantly Fermi-liquid-like temperature dependence in the coherent region. The dashed curve indicated in figure 2 for $CePt_2Si_2$ at low temperatures is a least-squares fit of the equation

$$\rho(T) = \rho_0 + AT^2 + BT^5 \tag{1}$$

against the experimental data. As usual ρ_0 indicates the effect of scattering of conduction electrons from lattice defects and impurities, AT^2 is a Fermi-liquid contribution and BT^5 presents the scattering due to phonons in the low-temperature limit. Fits were performed in the range $4\ \text{K} \leqslant T \leqslant 15$ K where the high-temperature limit is 10% of the Debye temperature $\theta = 146$ K of this compound [12]. The following values of the parameters were obtained: $\rho_0 = 286 \times 10^{-8}\ \Omega$ m, $A = 5 \times 10^{-10}\ \Omega\ \text{m K}^{-2}$ and $B = 2.6 \times 10^{-14}\ \Omega\ \text{m K}^{-5}$. It is seen that the contribution to $\rho(T)$ of Fermi-liquid origin is dominant for this material at low temperatures.

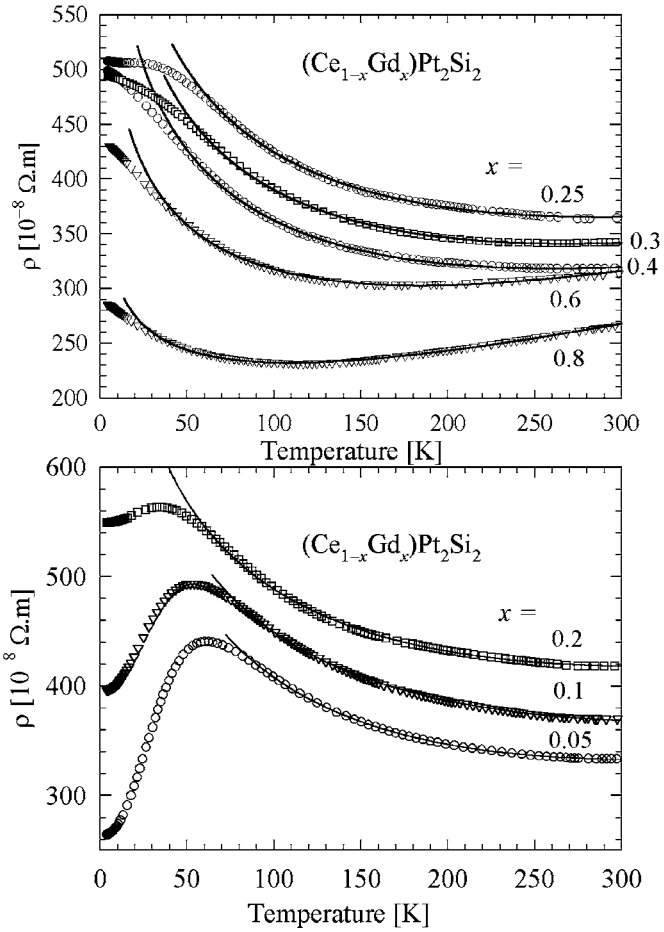

Figure 3. The temperature dependence of the electrical resistivity, $\rho(T)$, of the $(Ce_{1-x}Gd_x)Pt_2Si_2$ alloy series. The solid curves are least-squares fits of (2), which includes phonon and Kondo contributions to the resistivity, to the experimental data. The fit parameters are plotted in figure 4.

For $GdPt_2Si_2$ the resistivity decreases almost linearly over most of the studied temperature region indicating a normal metallic behaviour. As shown in the inset to figure 2 a small increase in $\rho(T)$ is observed for $GdPt_2Si_2$ below 12 K and this is followed by a peak at 8.5 K. Such a behaviour is reminiscent of the $\rho(T)$ curves of several rare-earth metals where it is attributed to the scattering of conduction electrons from the additional Brillouin zone boundaries that are introduced by antiferromagnetic (helical) ordering [18, 19]. Our measurements of magnetic susceptibility, $\chi(T)$, reported in section 3.3 strongly suggest the occurrence of antiferromagnetic order in $GdPt_2Si_2$ at a temperature $T_N = 10$ K. It is observed that the peak in $\rho(T)$ is at a lower temperature than T_N, which is in agreement with the behaviour observed in rare-earth metals [19]. Some structure is also seen in $\rho(T)$ below 6 K and is thought to correspond to an anomaly observed in $\chi(T)$ at a temperature $T_1 = 6.8$ K (see section 3.3).

Results of $\rho(T)$ for the $(Ce_{1-x}Gd_x)Pt_2Si_2$ series are depicted in figure 3. It is observed that the dominant $\rho(T)$ behaviour is that of both coherent and incoherent Kondo scattering for compounds with $0 \leqslant x \leqslant 0.2$ and incoherent Kondo scattering for compounds with $0.25 \leqslant x \leqslant 0.8$. Antiferromagnetic ordering is observed for compounds with $x = 1, 0.8$ and

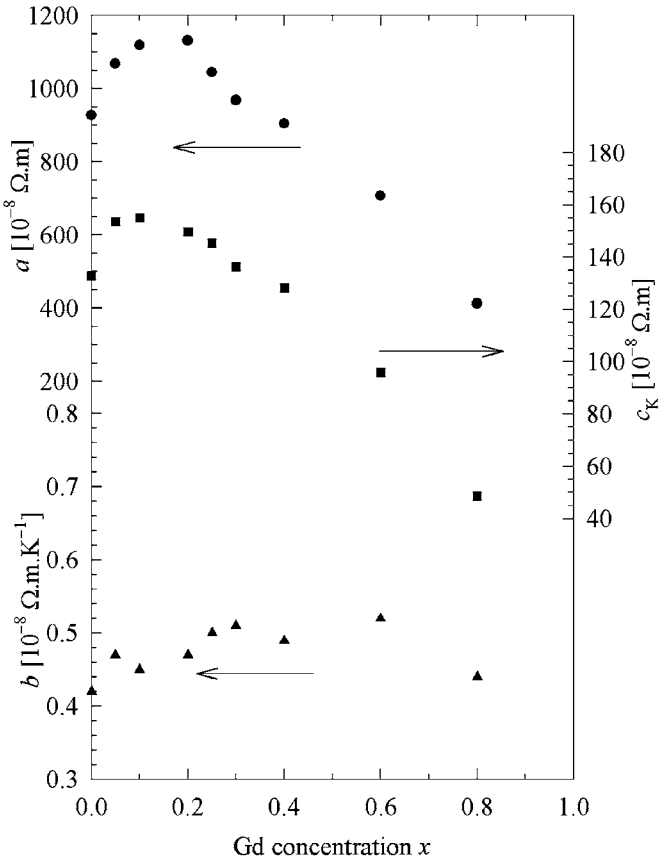

Figure 4. The dependence of the parameters a, b and c_K that describe the resistivity of the $(Ce_{1-x}Gd_x)Pt_2Si_2$ alloys in the incoherent Kondo region on the Gd concentration x.

0.6 at low temperatures (see section 3.3), but this has a very small effect on the resistivity. The higher-temperature incoherent Kondo behaviour of various $(Ce_{1-x}Gd_x)Pt_2Si_2$ alloys in figure 3 and of $CePt_2Si_2$ in figure 2 is hence described by

$$\rho(T) = \rho_0' + \rho_{ph}(T) + \rho_{mag}(T) \approx a + bT - c_K \ln(T). \tag{2}$$

The temperature independent term $\rho_0' = a$ accounts not only for the scattering of conduction electrons by lattice imperfections and impurities, but may also include a Nordheim-like contribution [20] due to the presence of two kinds of rare-earth atom (Ce and Gd) in the lattice. A small contribution due to spin-disorder resistivity for compounds with $x = 1$, 0.8 and 0.6 may be neglected ($<10^{-7}$ Ω m, see inset to figure 2). The phonon contribution is approximated as $\rho_{ph} \approx bT$ which is largely valid for the temperature region in which we fitted our data as is evident from the $\rho(T)$ curve of $GdPt_2Si_2$. The solid curves depicted in figures 2 and 3 result from least-squares fits of (2) against the experimental data. These yield values of a, b and c_K for the different alloys as plotted in figure 4. It is noted that the parameter a shows a weak maximum at small Gd concentration which indicates that this contribution is not completely of a Nordheim-like origin, $\rho_0 \sim x(1-x)$, which has a maximum at $x = 0.5$ [20]. The phonon coefficient b varies fairly smoothly as a function of the Gd concentration x. The incoherent Kondo scattering is described by c_K which, after a small initial increase, decreases

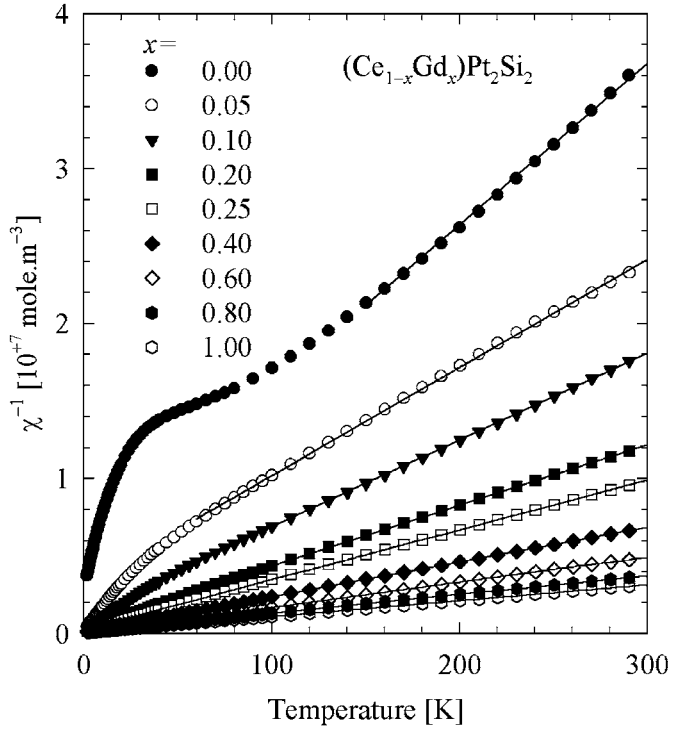

Figure 5. The temperature dependence of the inverse magnetic susceptibility for the alloy system $(Ce_{1-x}Gd_x)Pt_2Si_2$. The data refer to a mole of rare-earth atoms. The solid curves are fits of the Curie–Weiss law (3) to the data. The calculated parameters are given in table 1.

Table 1. Magnetic susceptibility data of the alloy system $(Ce_{1-x}Gd_x)Pt_2Si_2$. The effective magnetic moment, μ_{eff}, and the paramagnetic Curie temperature, θ_p, were obtained by a fit at higher temperature (see range) of the Curie–Weiss law (3) to the data as shown in figure 5. T_N values were obtained from figure 6.

x	T_N (K)	$-\theta_p$ (K)	μ_{eff} (μ_B)	Fit range (K)
1	10	7.1	7.89	10–300
0.8	7	6	7.21	10–300
0.6	4.5	4.8	6.27	20–300
0.4		5.5	5.32	28–300
0.25		8	4.45	30–300
0.2		11.1	4.03	40–300
0.1		23	3.37	50–300
0.05		46	3.2	60–300
0		53	2.47	150–300

with increase in Gd concentration x which is expected since the RKKY interaction becomes more important. It is nevertheless noted that, even with an 80% substitution of moment-bearing Gd, significant Kondo behaviour is retained in this system.

3.3. Magnetic susceptibility

Results of the inverse molar magnetic susceptibility, $\chi^{-1}(T)$, of $(Ce_{1-x}Gd_x)Pt_2Si_2$ with $0 \leqslant x \leqslant 1$ measured in a field of 0.5 T are shown in figure 5. Above a certain temperature, as

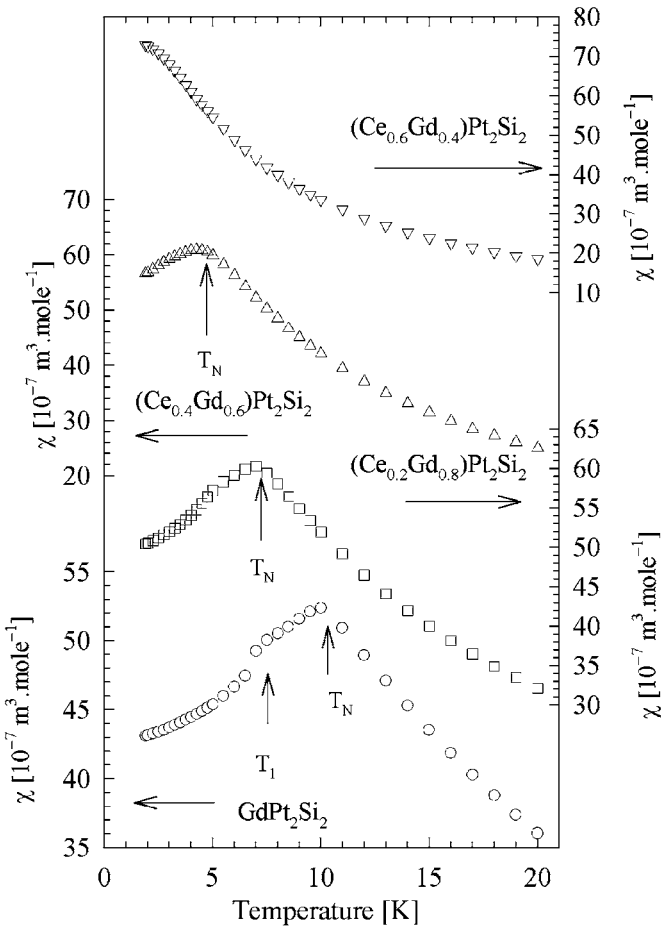

Figure 6. The temperature dependence of the susceptibility in the range 1.89 K $\leqslant T \leqslant$ 20 K for $(Ce_{1-x}Gd_x)Pt_2Si_2$ alloys, $0.4 \leqslant x \leqslant 1$. The data refer to a mole of rare-earth atoms. The arrows indicate the temperature below which antiferromagnetic ordering sets in (T_N) as well as another possible transition at T_1.

shown by the solid-curve fits, the reciprocal susceptibility follows a Curie–Weiss law

$$\chi^{-1}(T) = \frac{3k_B(T - \theta_p)}{N_A\mu_{eff}^2}, \tag{3}$$

where k_B is Boltzmann's constant and N_A is Avogadro's number. Values of the effective magnetic moment, μ_{eff}, the paramagnetic Curie temperature, θ_p, and the fit range employed are given in table 1. It is observed that the temperature range over which (3) is valid becomes progressively smaller as one progresses from the $GdPt_2Si_2$ compound to the $CePt_2Si_2$ compound. The μ_{eff} values observed for the two end-compounds are respectively almost equal to the expected free-ion values of 2.54 μ_B for Ce^{3+} and 7.94 μ_B for Gd^{3+}. A gradual increase in μ_{eff} is observed between $CePt_2Si_2$ and $GdPt_2Si_2$. This seems to indicate that at high temperatures the Ce and Gd ions contribute independently to the total moment. Roy *et al* [21] found a similar behaviour in $(Ce_xGd_{1-x})Cu_6$. Initially, $-\theta_p$ shows a very small decrease with substitution of Gd with Ce. This is followed by a very dramatic increase of $-\theta_p$ for the Ce-rich alloys ($0 \leqslant x \leqslant 0.25$), indicating the increase in the strength of Kondo interaction.

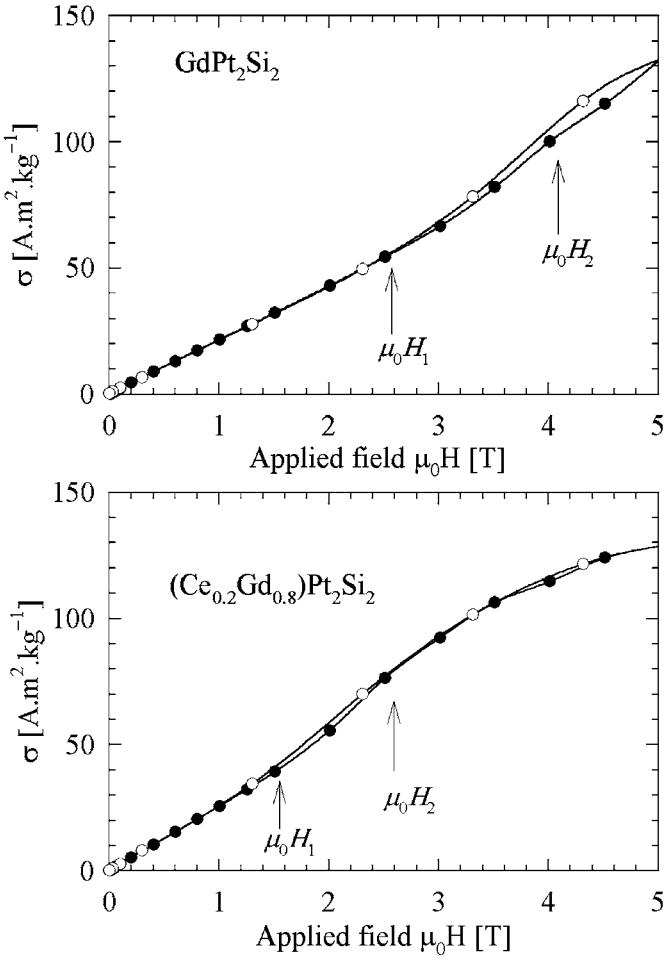

Figure 7. The field variation of the magnetization at 1.89 K for Gd-rich alloys with increasing (close symbols) and decreasing field (open symbols). The arrows indicate inflection points and these are associated with metamagnetic transitions.

In figure 6 the low-temperature magnetic susceptibility is shown for the temperature range 1.89 K $\leqslant T \leqslant$ 20 K for alloys with $0.4 \leqslant x \leqslant 1$. For alloys with $x \geqslant 0.6$, the susceptibility displays an antiferromagnetic peak at the Néel temperature, T_N, as indicated by the arrows in figure 6. In the case of $GdPt_2Si_2$, the $\chi(T)$ curve furthermore shows a step at a lower temperature T_1, which is interpreted as a further phase transition since an anomaly near this temperature is also evident in the $\rho(T)$ results. The observed values of T_N are given in table 1 and are seen to decrease with decreasing Gd content. The magnitude of the susceptibility at and below T_N increases with decreasing Gd content x.

3.4. Magnetization

The field dependence of the magnetization, σ, for alloys of the $(Ce_{1-x}Gd_x)Pt_2Si_2$ series is displayed in figures 7 and 8. In figure 7 it is seen that the $GdPt_2Si_2$ and $(Ce_{0.2}Gd_{0.8})Pt_2Si_2$ samples show complex magnetic behaviour. There is a clear departure from a linear σ versus $\mu_0 H$ behaviour observed at lower fields through an upward increase in σ above $\mu_0 H_1$ values

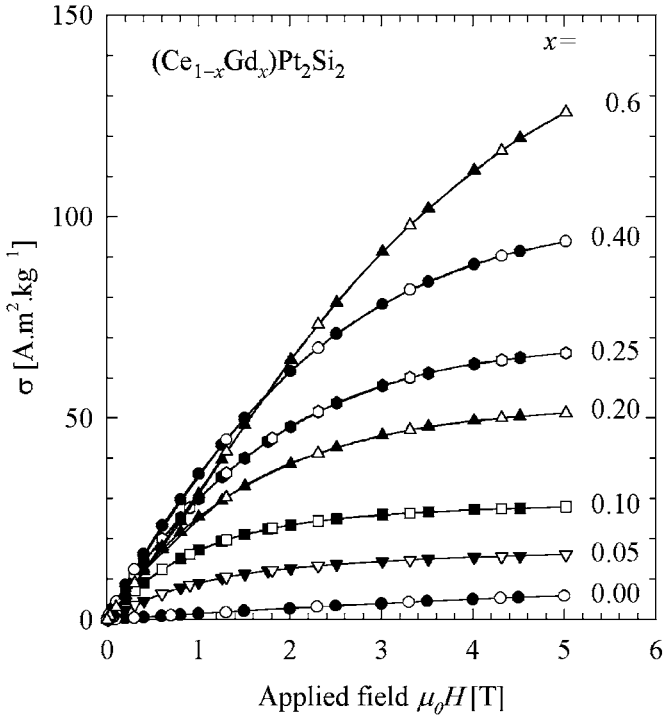

Figure 8. The field variation of the magnetization at 1.89 K for $(Ce_{1-x}Gd_x)Pt_2Si_2$ alloys with $0 \leqslant x \leqslant 0.6$ for increasing (closed symbols) and decreasing field (open symbols).

as indicated in figure 7. The magnetization in the higher-field region shows hysteresis effects and a further inflection point at field values $\mu_0 H_2$ as indicated. These characteristics suggest metamagnetic behaviour, the details of which may be more clearly evident if studies on single-crystal samples can be carried out. The magnetization of the other $(Ce_{1-x}Gd_x)Pt_2Si_2$ alloys (figure 8) departs from a linear behaviour in relatively small fields and is distinctly curved with a tendency towards saturation for the maximum applied field of 5 T. Magnetization studies on $(Ce_{1-x}Gd_x)Al_3$ [22, 23] also indicate antiferromagnetism for Gd concentration above 0.6, but in addition report spin-glass-like behaviour.

4. Conclusion

The present study of $(Ce_{1-x}Gd_x)Pt_2Si_2$ alloys indicates the evolution from Kondo lattice, through incoherent single-ion Kondo to magnetically ordered behaviour as x is increased. Alloys with $x \geqslant 0.6$ exhibit antiferromagnetism and for the $x = 0.8$ and 1.0 samples the magnetization results suggest metamagnetic behaviour.

Acknowledgments

Financial support by the South African National Research Foundation (NRF) under grant number 2053778 and by the University of the Witwatersrand Research Committee is acknowledged. The work at the Institute of Low Temperature and Structure Research, Wroclaw, was supported by the State Committee for Scientific Research (KBN) within grant

number 4 T08A 045 24. Mr R Gorzelniak is thanked for valued technical assistance. Any opinion, findings and conclusions or recommendations expressed in this paper are those of the authors and do not necessarily reflect the views of the NRF.

References

[1] Rogl P 1984 *Handbook on the Physics and Chemistry of Rare Earths* vol 7, ed K A Gschneidner Jr and L Eyring (Amsterdam: Elsevier) ch 51 p 1
[2] Dommann A, Hulliger F, Ott H R and Gramlich V 1985 *J. Less-Common Met.* **110** 331
[3] Hiebl K and Rogl P 1985 *J. Magn. Magn. Mater.* **50** 39
[4] Palstra T T M, Menovsky A A, Nieuwenhuys G J and Mydosh J A 1986 *J. Magn. Magn. Mater.* **54–57** 435
[5] Gignoux D, Schmitt D, Zerguine M, Ayache C and Bonjour E 1986 *Phys. Lett.* A **117** 145
[6] Rossi D, Marazza R and Ferro R 1979 *J. Less-Common Met.* **66** 17
[7] Ayache C, Beille J, Bonjour E, Calemczuk R, Creuzet G, Gignoux D, Najib A, Schmitt D, Voiron J and Zerguine M 1987 *J. Magn. Magn. Mater.* **63/64** 329
[8] Marsolais R M, Ayache C, Schmitt D, Bhattacharjee A K and Coqblin B 1988 *J. Magn. Magn. Mater.* **76/77** 269
[9] Rajan V T 1983 *Phys. Rev. Lett.* **51** 308
[10] Bhattacharjee A K, Coqblin B, Raki M, Ferro L, Ayache C and Schmitt D 1989 *J. Physique* **50** 2781
[11] Steeman R A, Dirkmaat A J, Menovsky A A, Frikkee E, Nieuwenhuys G J and Mydosh J A 1990 *Physica* B **163** 382
[12] Dalmas de Réotier P, Yaouanc A, Calemczuk R, Huxley A D, Marcenat C, Bonville P, Lejay P, Gubbens P C M and Mulders A M 1997 *Phys. Rev.* B **55** 2737
[13] Gignoux D, Schmitt D and Zerguine M 1988 *Phys. Rev.* B **37** 9882
[14] Gignoux D, Schmitt D, Zerguine M and Murani A P 1988 *J. Magn. Magn. Mater.* **76/77** 401
[15] Bouziane K and du Plessis P de V 1999 *J. Phys.: Condens. Matter* **11** 3161
[16] Tchoula Tchokonté M B, du Plessis P de V, Strydom A M and Kaczorowski D 2001 *J. Magn. Magn. Mater.* **226–230** 173
[17] Lavagna M, Lacroix C and Cyrot M 1982 *J. Phys. F: Met. Phys.* **12** 745
[18] Miwa H 1962 *Prog. Theor. Phys.* **28** 208
Miwa H 1962 *Prog. Theor. Phys.* **29** 477
[19] Elliott R J and Wedgwood F A 1963 *Proc. Phys. Soc.* **81** 846
Elliott R J and Wedgwood F A 1963 *Proc. Phys. Soc.* **84** 63
[20] Blatt F J 1968 *Physics of Electronic Conduction in Solids* (New York: McGraw-Hill)
[21] Roy S B, Lees M R, Stewart G R and Coles B R 1991 *Phys. Rev.* B **43** 8264
[22] Edelstein A S and Holtz R L 1988 *J. Appl. Phys.* **63** 3689
[23] Edelstein A S, Holtz R L, Gillespie D J, Rubinstein M, Tyson J, Fisher R A and Phillips N E 1988 *Phys. Rev.* B **37** 7877